This is a draft version. Please cite it as: Chen, D., Laval, J., Ahn, S., Zheng, Z., 2012. Microscopic traffic hysteresis in traffic oscillations: a behavioral perspective. *Transportation Research Part B 46*(10), 1440-1453.

Traffic Hysteresis in Traffic Oscillations: A Behavioral Perspective

Abstract:

This paper studies traffic hysteresis arising in traffic oscillations from a behavioral perspective. It is found that the occurrence and type of traffic hysteresis is closely correlated with driver behavior when experiencing traffic oscillations and with the time driver reaction begins relative to the starting deceleration wave. Statistical results suggest that driver behavior is different depending on its position along the oscillation. This suggests that different car-following models should be used inside the different stages of an oscillation in order to replicate realistic congestion features.

Keywords: Traffic oscillations, Car-following behavior, Traffic hysteresis, Generation mechanism

1 Introduction

Traffic hysteresis in freeway traffic was first explicitly observed in 1974 (Treiterer and Myers, 1974). It was found that the relationship between density and speed (and also volume) from a platoon of vehicles that underwent disturbances on a freeway exhibited obvious loops. Similar hysteresis loops were found from transient traffic conditions after incidents (Maes, 1979). Generally, traffic hysteresis is characterized with retardation in speed recovery. Although traffic hysteresis has been observed over decades, our understanding on its occurrence is still very limited.

Several theories and models have been proposed to explain traffic hysteresis. Newell (1965) conjectured that hysteresis arise due to the asymmetry between acceleration and deceleration, which leads to two congested branches on a fundamental diagram. Zhang (1999) formulated the asymmetry mathematically. He used three traffic phases to describe traffic flow: acceleration, deceleration, and strong equilibrium phase, and showed that the transition of the speed-density relationship in different phases could form hysteresis loops. Some of the predictions from his traffic theory accorded well with empirical data. Zhang and Kim (2005) proposed a car-following model in which the speed of a driver was determined by the traffic phase and the gap-time (time required to get to the leader's rear position). When certain functions are used for the variable, gap-time, their model could produce traffic hysteresis, but the model was not tested on empirical data. Yeo and Sakabardonis (2009) divided traffic conditions into five states: free-flow, acceleration, deceleration, coasting and stationary, and argued that the acceleration and deceleration processes were asymmetric, which caused traffic hysteresis. However, according to their theory counter clock-wise hysteresis loop will not be produced, which is not consistent with field observations. These models describe traffic hysteresis as a result of asymmetry in different traffic phases. However, the underlying root of asymmetry is unknown. Another hypothesis emerges recently, which argues that traffic hysteresis may be explained by the heterogeneous composition of driver population (Wong and Wong, 2002; Ngoduy, 2011), and some of the simulation results show traffic hysteresis (e.g., Wong and Wong, 2002). For example, Wong and Wong (2002) extended the kinematic wave model (Lighthill and Whitham, 1955; Richards, 1956) to multiple classes and assumed that each class follows one density-speed relationship. Their simulations generated a macroscopic clockwise traffic hysteresis loop. These studies are macroscopic exploration in a conjecture state. Additionally, no explanation was provided for the existence of counter clockwise hysteresis loop.

Laval (2010) and Ahn, et al. (2011) argued that the magnitude of hysteresis has been over-estimated in previous studies because of measurements taken during non-steady state conditions. All previous references may be subject to measurement bias. To overcome this problem, Laval (2010) took measurements on regions of (near) steady states (i.e., stationary or stationary non-equilibrium traffic states) from vehicle trajectory data using Edie's generalized definition of flow, density, and speed (Edie, 1961). Ahn et al. (2011) measured the evolution of speed-spacing relations as vehicles underwent stop-and-go oscillations. To account for the non-steady conditions, instead of the observed spacing, they measured the equilibrium spacing projected from the kinematic wave model (Lighthill and Whitham, 1955; Richards, 1956) with a triangular fundamental diagram. These studies found that the magnitude of hysteresis is not as significant as previously thought. Nevertheless, hysteresis was still present (in smaller frequency and magnitude) in the observations. In addition, reverse hysteresis loops were found in both studies (Laval, 2010), although its proportion was smaller (Ahn et al., 2011).

This is a draft version. Please cite it as: Chen, D., Laval, J., Ahn, S., Zheng, Z., 2012. Microscopic traffic hysteresis in traffic oscillations: a behavioral perspective. *Transportation Research Part B 46*(10), 1440-1453.

In most of the empirical and theoretical studies cited above, traffic hysteresis was not investigated with a behavioral perspective. In the few studies that mentioned driver behavior (Newell, 1965; Yeo and Skabardonis, 2009, Wong and Wong, 2002), the connection between traffic hysteresis and driver behavior was in a state of conjecture and was not investigated extensively. For example, in Newell' conjecture (Newell, 1965), the driving rules resulted in the asymmetry between the acceleration and deceleration branches. According to Yeo and Sakabardonis (2009), human errors such as maneuvering errors and anticipation might be associated with the state transition, but the relationship between human errors and traffic hysteresis was not investigated. Nevertheless, the connection between hysteresis and driver behavior is still not clear. Recent studies (Chen et al., 2012; Laval and Leclercq, 2010) reveal that traffic oscillations, with which traffic hysteresis is usually associated, may have strong connection with driver behavior. Particularly, Laval and Leclercq (2010) attributed the formation and propagation of traffic oscillations to the aggressive or timid behavior of drivers in their model. Chen, et al. (2012) provided empirical evidence to confirm the connection and proposed an asymmetric behavioral model to capture driver behavior throughout traffic oscillations in congestion. Simulations from both studies were able to produce traffic oscillations consistently with empirical observation.

Based on these results, this paper studied traffic hysteresis arising in traffic oscillations from a behavioral perspective. The remainder of the paper is organized as follows: Section 2 describes the data used and Section 3 introduces the background for car-following driver behavior and traffic hysteresis. Section 4 presents the methodology for measurement. Statistical results are provided in Section 5. Further insights based on the statistical results are presented in Section 6. Conclusions and discussions are provided in Section 7.

2 Data

This paper uses the vehicle trajectory data for the US-101 site provided by the Next Generation Simulation project (NGSIM, 2006). The data was collected on a 6-lane 2100-foot segment southbound of US-101 in Log Angles, California (see Figure 1(a) for the sketch) from 7:50 -8:35 a.m. on June 15, 2005. We only use the data of lane 1 from 7:50-8:05 a.m. because oscillations formed spontaneously with the fewest lane-changing maneuvers; see Figure 1(b). Notice that traffic oscillations spontaneously arise every 2-3 minutes and fully-develop to a (near) complete stop as they propagate upstream (see Figure 1(b)).

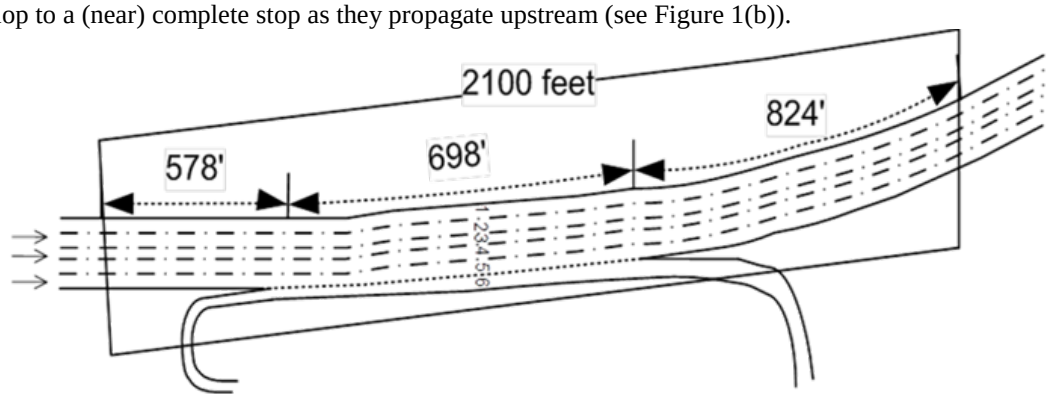

(a)

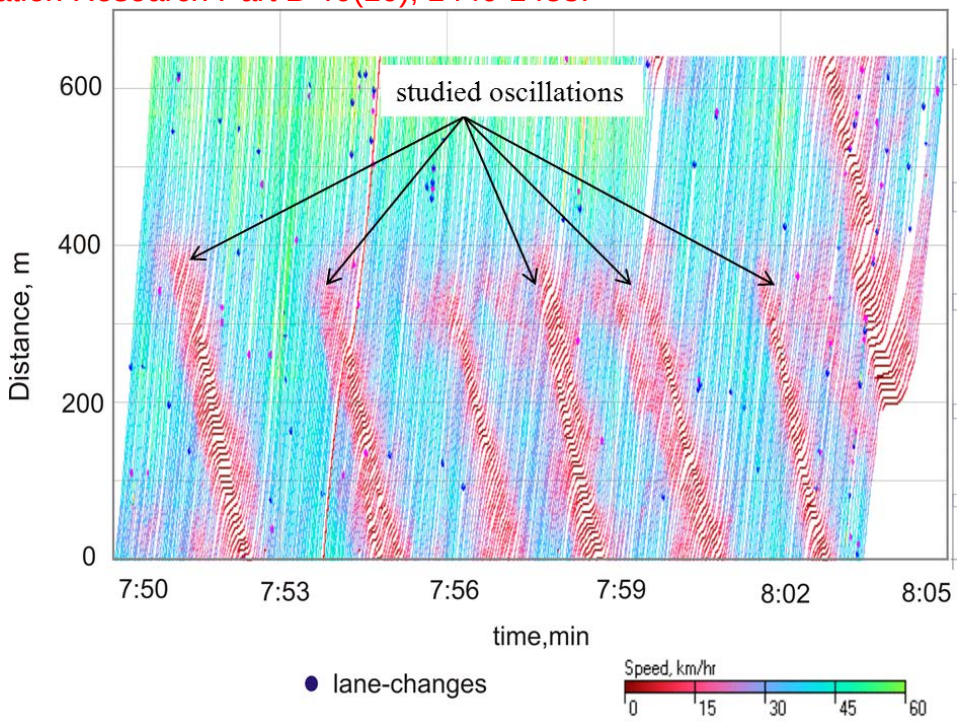

(b)

Figure 1 (a) schematic of US-101 study site; (b) trajectory data (US 101 lane 1).

We have selected five traffic oscillations (shown in the figure) that arise spontaneously and fully develop as they propagate upstream to analyze traffic hysteresis. Notice that oscillations that are short-lived are not included. Measurements were conducted on leader-follower trajectory pairs. Trajectories in the vicinity of lane-changing maneuvers were excluded to avoid the compound effects.

3 Background

Newell's car-following model (Newell, 2002) captures the relationship between speed and spacing, which is explained by Figure 2. This model is simple but is appealing because it gives the exact numerical solution to the kinematic wave model (Lighthill and Whitham, 1955; Richards, 1956) with a triangular fundamental diagram (KWT model). In this model, the trajectory of a driver in congestion is a translation of the leader's by a time shift τ and space shift d. The variable τ is the wave trip time between two consecutive drivers and d is the jam spacing. For a specific driver, driver i, the two variables (τ, d) are denoted as (τ_i, d_i). In this model (τ_i, d_i) remains constant for a given driver but may vary across drivers. Notably, these two parameters can be written using parameters of the KWT model:

$$\tau = \frac{1}{w\kappa} \text{ and } d = \frac{1}{\kappa},$$

where $-w$ is wave speed and κ is jam density.

Laval and Leclercq (2010) observed that driver i may have (τ_i, d_i) deviate from constant value. To capture the deviation, a variable $\eta_i(t)$, defined as

$$\eta_i(t) = \tau_i(t)/\tau, \tag{1}$$

is used, where $\tau_i(t)$ is the actual wave travel time of driver i at time t and τ is the equilibrium value derived from the KWT model. The wave speed is assumed to be constant. Thus, the term $\eta_i(t)$ is sufficient to capture

the dynamics of the two parameters (τ_i, d_i) because $d = \tau w$. Notice that $\eta_i(t)$ is equivalent to the ratio of the actual steady spacing to the equilibrium spacing.

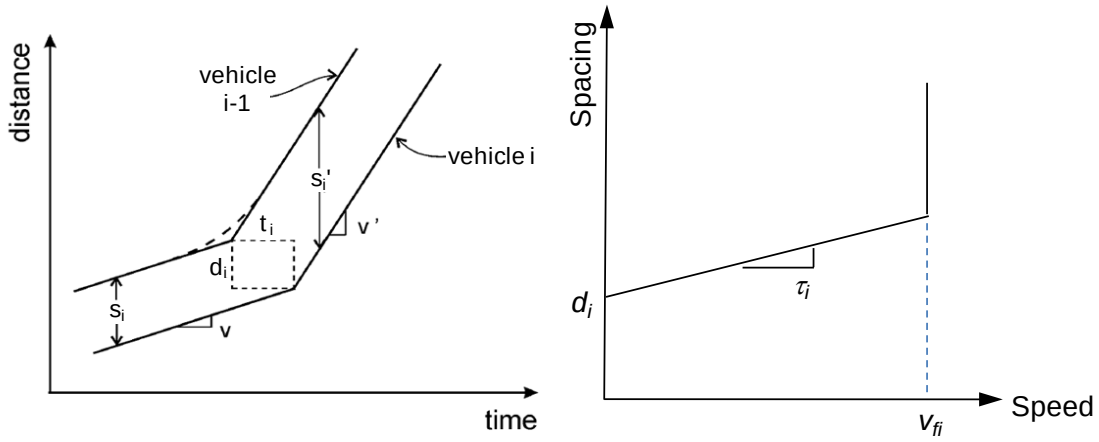

Figure 2 (a) Illustration of Newell's Car-following Theory; (b) Speed-spacing relationship based on Newell's car following Theory.

Based on empirical observations, Chen, et al. (2012) proposed an asymmetric behavioral model to describe driver's car-following behavior throughout a traffic oscillation, which was extended from a model of Laval and Leclercq's (2010). According to the asymmetric behavioral model, drivers maintain constant $\eta_i(t)$-value when they are in equilibrium, but in non-equilibrium, which is triggered whenever the deceleration wave of an oscillation starts, $\eta_i(t)$ deviates from the constant value. Figure 3 shows an empirical driver profile, in which η_i^0 (η_i^1) refers to the stable value of $\eta_i(t)$ before (after) the non-equilibrium, and η_i^T is the value when the vehicle has the maximum deviation from η_i^0. Clearly, the η_i^0-value captures the congestion equilibrium branch that a driver prefers to maintain before an oscillation; i.e., it is a driver characteristic. When η_i^0 equals to 1, the behavior of driver i accords well with the theoretical fundamental diagram of the KWT model. Hence, the η_i^0-value is used to define driver category: originally aggressive (OA) if $\eta_i^0 \ll 1$, originally timid (OT) if $\eta_i^0 \gg 1$, and originally Newell (ON) if $\eta_i^0 \sim 1$.

The asymmetric behavior model also uses reaction pattern to capture driver behavior in non-equilibrium, which manifests driver's response to an oscillation. The reaction pattern is approximated by three cases: concave triangle ($\eta_i^T > \eta_i^0$ & $\eta_i^T > \eta_i^1$) , convex triangle ($\eta_i^T < \eta_i^0$ & $\eta_i^T < \eta_i^1$), and constant ($\eta_i^T \sim \eta_i^0 \sim \eta_i^1$). The triangles are not necessarily isosceles or symmetric; i.e., $\varepsilon_i^0 <> \varepsilon_i^1$ and $\eta_i^T <> \eta_i^1$ where ε_i^0 (ε_i^1) is the average slope of $\eta_i(t)$ between η_i^0 (η_i^T) and η_i^T (η_i^1). The beginning and ending points of the response to an oscillation are denoted by t^0 and t^1, respectively. Notice that the response refers to the change of $\eta_i(t)$ rather than the physical action such as acceleration or deceleration.

This is a draft version. Please cite it as: Chen, D., Laval, J., Ahn, S., Zheng, Z., 2012. Microscopic traffic hysteresis in traffic oscillations: a behavioral perspective. *Transportation Research Part B 46*(10), 1440-1453.

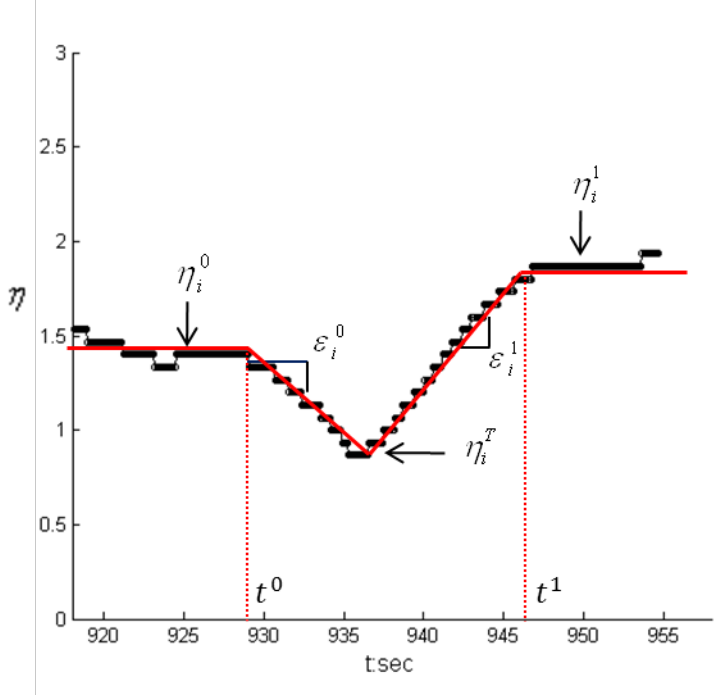

Figure 3 Asymmetric behavioral model

4 Measurement

4.1 Driver Behavior Measurement

We use the model proposed by Chen, et al. (2012) to represent driver behavior throughout traffic oscillations. Thus, the measurement of $\eta_i(t)$ is given by Equation (1), which can be boiled down to measuring $\tau_i(t)$. Since $\tau_i(t)$ depends on the wave speed w we set a range -5ft/s~20ft/s for w as reported in the literature (Chen et al., 2012; Durent et al., 2011; Laval and Leclercq, 2010) and select the value that minimizes the variance of the $\tau_i(t)$ time series; i.e., that fits Newell's car-following model best. As a result, the wave speed used in the measurement is fixed for a given driver but it varies across drivers. With a given wave speed, we measure the trip time $\tau_i(t)$ along the follower's trajectory and obtain a time series of $\tau_i(t)$ as illustrated in Figure 4. The equilibrium value τ is set to be the mean of $\tau_i(t)$ before oscillations from all trajectories sampled.

This is a draft version. Please cite it as: Chen, D., Laval, J., Ahn, S., Zheng, Z., 2012. Microscopic traffic hysteresis in traffic oscillations: a behavioral perspective. *Transportation Research Part B 46*(10), 1440-1453.

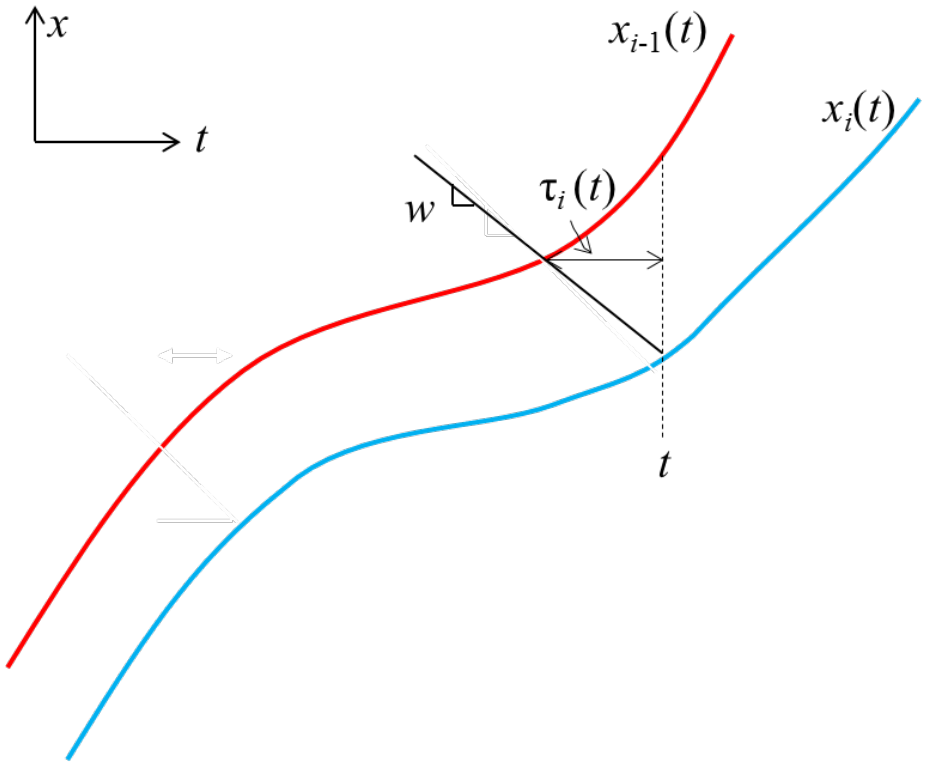

Figure 4 Measurement of $\boldsymbol{\tau_i(t)}$.

The reaction patterns used in this paper are: concave, convex, non-decreasing, and constant. Note that the triangular-shape approximation for concave and convex is not required. Additionally, the non-decreasing pattern is added to capture the case shown in Figure 5 (a-b), where $\eta_i(t)$ increases until reaching η_i^T but it has no obvious decrease thereafter; i.e., $\eta_i^1 <> \eta_i^T$. In most of the non-decreasing cases observed, $\eta_i(t)$ remains stable after reaching η_i^T as in the case of Figure 5(a), which appears similar to the concave pattern. However, we find it necessary to distinguish these two patterns when explaining the occurrence of traffic hysteresis. This will be revisited later.

Similarly to Chen, et al. (2012), we set the threshold to be $\eta_i^0 < 0.9$ for OA drivers, $\eta_i^0 > 1.1$ for OT drivers and $0.9 \leq \eta_i^0 \leq 1.1$ for ON drivers.

This is a draft version. Please cite it as: Chen, D., Laval, J., Ahn, S., Zheng, Z., 2012. Microscopic traffic hysteresis in traffic oscillations: a behavioral perspective. *Transportation Research Part B 46*(10), 1440-1453.

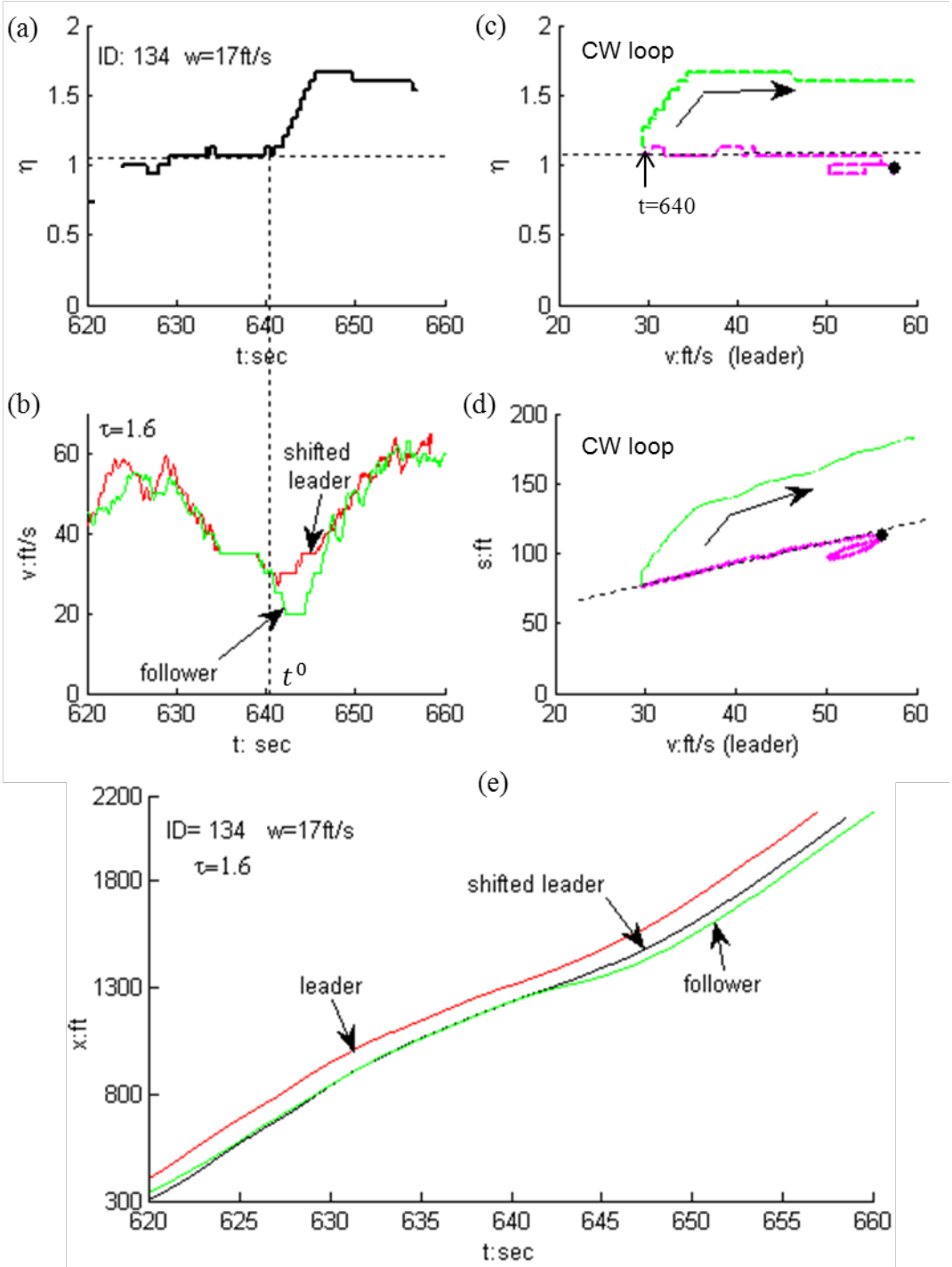

Figure 5 (a) $\eta_i(t)$ plot for the non-decreasing pattern; (b) Corresponding speed plot throughout an oscillation (leader's trajectory is shifted to the right by τ) ; (c) η_i versus speed plot; (d) Spacing versus speed.

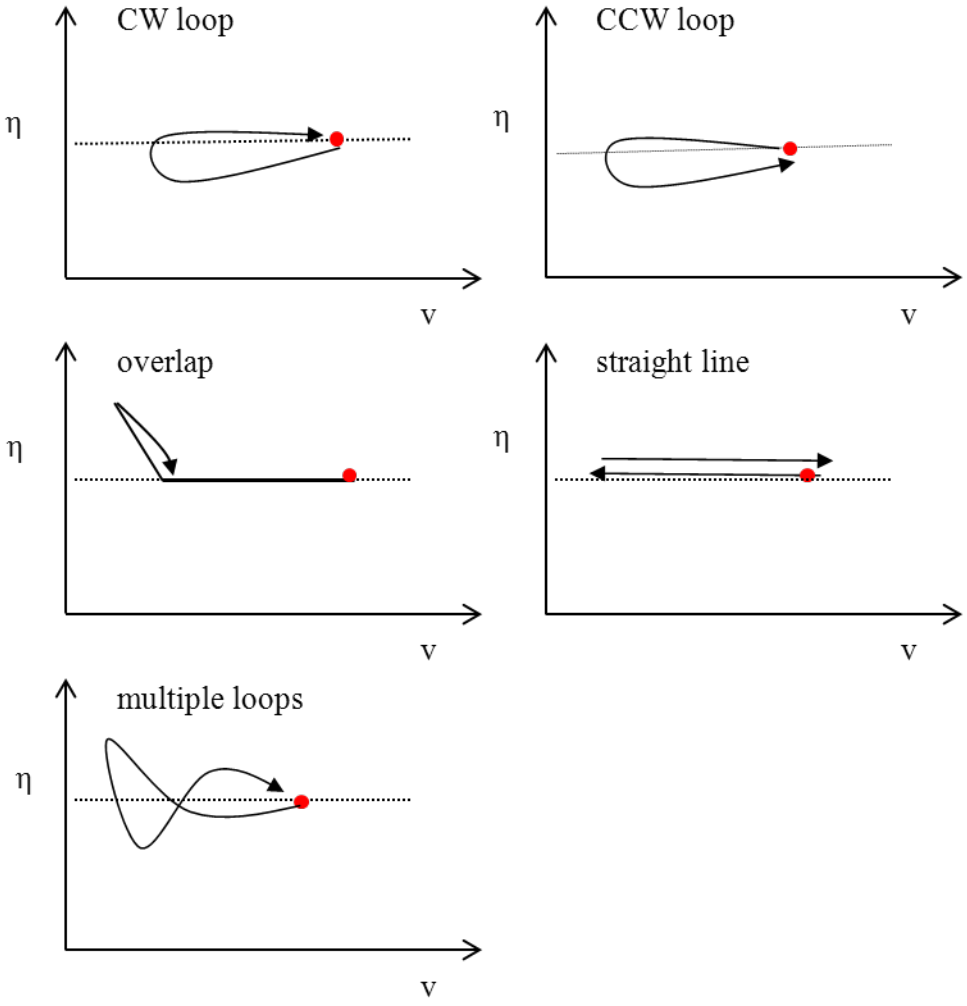

Figure 6 Hysteresis cases (red dot: beginning of hysteresis loop; dash lines are from Newell's car-following model)

4.2 Measurement of Traffic Hysteresis

We analyze traffic hysteresis on the $v-\eta$ plane so that driver category, reaction pattern, and traffic hysteresis can be captured simultaneously. Note that since $\eta_i(t)$ is the ratio of the actual steady spacing to the equilibrium spacing, the hysteresis orientation in the $v-\eta$ plot is the same as in the speed-density ($v-s$) plot, and the flow-density plot; see Figure 5 (c-d). We define five hysteresis types according to the orientation of the $v-\eta$ curves during an oscillation cycle: clock-wise (CW) loop, counter clock-wise (CCW) loop, overlap, straight line, and multiple loops. This is illustrated in Figure 6 where the red dots denote the beginning of the $v-\eta$ plots and the arrows show the orientation. All the cases except for the overlap case are self-explanatory. In the overlap case, the $v-\eta$ relationship deviates from Newell's prediction but is identical in the deceleration and acceleration processes. Although hysteresis is not significant in the overlap and straight line cases, we include them to obtain a more comprehensive description. The CW and CCW loops in this paper correspond to the hysteresis and reverse hysteresis loops respectively in the literature (Laval, 2010).

4.3 Development Stage of Oscillations

An oscillation is broken down into two periods to capture the potential change of driver behavior and traffic hysteresis in different development stages of an oscillation.

In the growth period, the minimum speed of drivers during an oscillation cycle *decreases* as the oscillation propagates upstream.

In the fully-developed period the minimum speed of drivers during an oscillation cycle *stops decreasing*.

Figure 7 provides an illustration for the period setting. The red solid line approximates the trend of minimum speed across vehicles in an oscillation. As one can see, the minimum speed tends to decrease until it becomes close to 0 and then remains stable. Hence, the black point denotes the threshold and vehicles before (after) it fall into the growth (fully-developed) period.

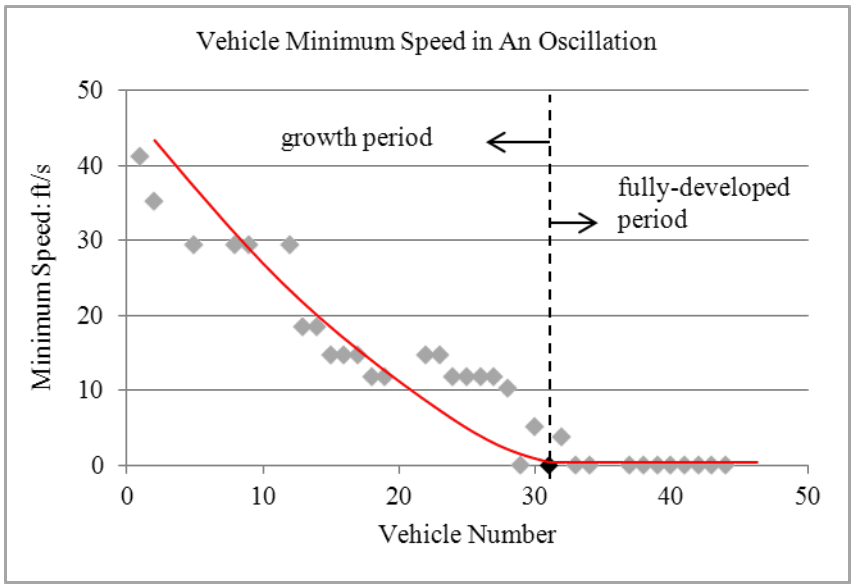

Figure 7 Minimum Speed of Vehicles along A Traffic Oscillation

5 Statistical Results

This section presents statistical results of the three key elements, hysteresis pattern, driver category, and reaction pattern.

We use the chi-square test for homogeneity of proportions (Greenwood and Nikulin, 1996) to assess whether the distribution of a categorical variable (e.g., reaction pattern) from different populations are significantly different, at a 95% confidence level.

A total of 109 and 126 trajectory pairs were measured for the growth and fully-developed periods, respectively. Major remarks from the statistical results are summarized as follows.

R1: Drivers in the two periods come from the same distribution. The composition of driver category is not significantly different in the two periods (at the 5% level of significance) (p-value =0.32).

R2: About 60~75% of drivers show CW or CCW loops in the two periods (see Figure 8), but the distribution of hysteresis types in the two periods differs significantly (at the 5% level of significance) (p-value <0.001). CW loops are prevalent in the growth period, while the proportions of CW and CCW loops are comparable in the fully-developed period. The frequency of hysteresis types is shown in Table 1.

R3: Changes in reaction pattern preference between growth and fully-developed periods; see Figure 9 and the frequency distribution in Table 2 and Table 3:

R3a: OA drivers have significantly different reaction pattern preference (at the 5% level of significance) (*p*-value <0.001). In the growth period, they tend to adopt both concave and non-decreasing patterns but mainly adopt the concave pattern in the fully-developed period.

R3b: ON drivers also have significantly different preferences (at the 5% level of significance) (*p*-value =0.033). They have comparable probabilities to adopt any of the four reaction patterns in the growth period but a marked preference for the concave pattern in the fully-developed period.

R3c: The preference of OT drivers has no significant change (at the 5% level of significance) in the two periods (*p*-value =0.972). They consistently prefer the convex pattern.

R3d: For all driver categories combined, the distribution of reaction pattern is significantly different (at the 5% level of significance).

R3e: The distribution of reaction pattern for any two driver categories differs significantly (at the 5% level of significance); i.e., we cannot further reduce the number of driver category.

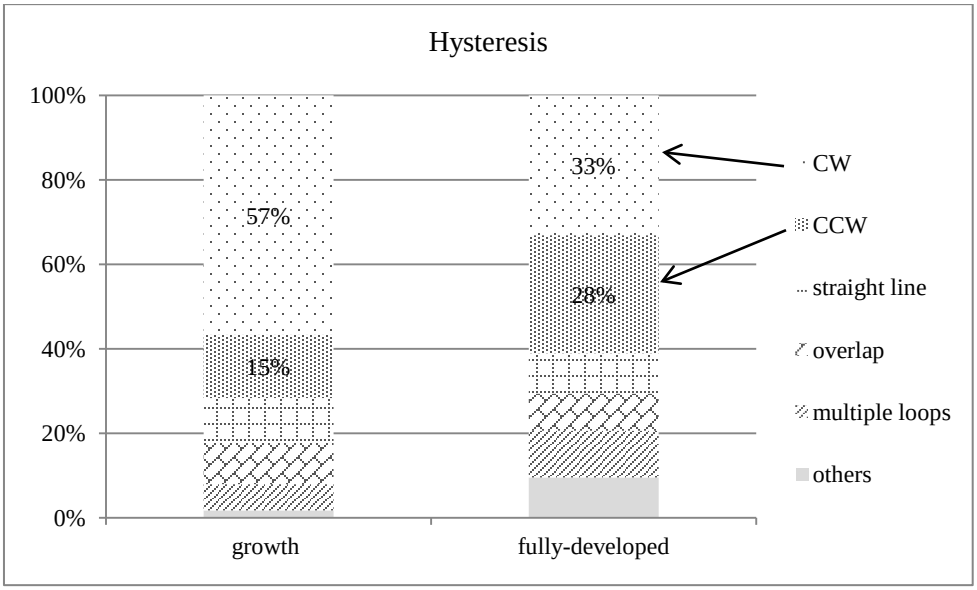

Figure 8 Composition of hysteresis patterns

Table 1 Distribution of Hysteresis Pattern

	CCW loop	straight line	CW loop	overlap	multiple loop*	others*
Growth	17	12	64	11	7	2
Fully-developed	38	13	45	12	15	13

*note: the two categories, multiple loop and others, are combined in chi-square test to meet the frequency requirement.

Table 2 Driver Category vs. Reaction Pattern

OT	Period	convex	others	
p-value	Growth Period	18	13	
0.972	Fully-developed Period	16	13	
ON		convex	concave	others
p-value	Growth Period	9	8	16
0.033	Fully-developed Period	9	27	15

This is a draft version. Please cite it as: Chen, D., Laval, J., Ahn, S., Zheng, Z., 2012. Microscopic traffic hysteresis in traffic oscillations: a behavioral perspective. *Transportation Research Part B 46*(10), 1440-1453.

OA		concave	others	
p-value	Growth Period	17	32	
<0.001	Fully-developed Period	45	11	

*note: some categories are combined to meet the frequency requirement. Frequency of each category is in Table 3.

Table 3 Frequency of Each Reaction Pattern

OT	concave	convex	non-decreasing	constant	others
growth period	4	18	4	4	1
fully-developed period	7	16	0	2	4
ON	concave	convex	non-decreasing	constant	others
growth period	8	9	11	4	1
fully-developed period	27	9	3	7	5
OA	concave	convex	non-decreasing	constant	others
growth period	17	7	20	3	2
fully-developed period	45	0	8	2	1

Remark R1 is intuitive because driver category is a driver characteristic and one does not expect it to vary with the development stage of traffic oscillations. This result eliminates potential variance caused by different driver samples in this study. In R2, the total proportion of CW and CCW loops is consistent with results of Ahn, et al. (2011) and Laval (2010). However, the significant change of hysteresis type distribution across the two periods is surprising. Given R1, we suspect this change is related to results in R3, which suggests that driver behavior may vary with the development stage of an oscillation. Examination on the relationship between the composition of hysteresis types (CW and CCW loop), driver category, and reaction pattern indicates that statistical analysis is not sufficient to unveil the complex connections. Therefore, we conduct more thorough investigation on vehicle trajectories in the next section to explore the relationship.

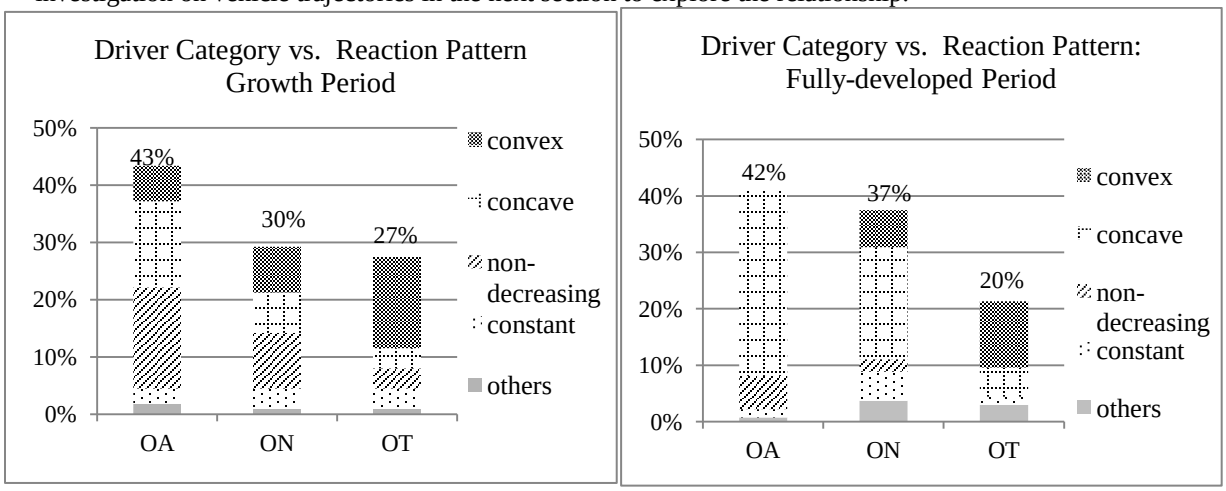

Figure 9 (a) Driver category vs. reaction pattern in growth period; (b) Driver category vs. reaction pattern in fully-developed period.

This is a draft version. Please cite it as: Chen, D., Laval, J., Ahn, S., Zheng, Z., 2012. Microscopic traffic hysteresis in traffic oscillations: a behavioral perspective. *Transportation Research Part B 46*(10), 1440-1453.

6 Analyses

In this section, we study the mechanism of generating traffic hysteresis in oscillatory traffic with the objective to explain the statistical results described in Section 5. We first analyze the potential cases that traffic hysteresis can be generated and then show the major mechanisms suggested by our empirical results. Afterwards, we explain the distribution change of traffic hysteresis types in the growth and fully-developed periods.

6.1 Potential traffic hysteresis

It is found that the different reaction patterns are correlated with the different types of hysteresis loops. Illustrations of some common cases are shown in Figure 10 in which the red dots denote the starting point and the arrows show the orientation of $\eta(t)$. For a concave pattern, if the increase-decrease change of $\eta(t)$ occurs and is completed within the deceleration process, a CCW loop is generated (see case "1" in Figure 10 (a)); if the change starts and ends within the acceleration process, the loop is CW; see "2" in Figure 10 (a). If the change spreads across the whole cycle, multiple loops are possible (see case "3"). Apparently, if the changes in $\eta(t)$ are symmetric on the $v-\eta$ plane, the trajectory pair causes the overlap hysteresis type (see case "1" in Figure 10 (d)). Similar analysis applies to the convex pattern (see Figure 10 (b) and case "2" in Figure 10(d)). For the non-decreasing pattern, because $\eta(t)$ is non-decreasing in an oscillation cycle as speed decreases and increases, the acceleration branch of $v-\eta$ plot will always be above the deceleration branch, which consequently determines the CW orientation (see Figure 10 (c)). Of course, the hysteresis in this case is not a loop in a strict sense because the curve does not close. Since our primary concern is the orientation, we still refer to it as the CW loop.

One can see that as long as the change in $\eta(t)$ is not symmetric on the $v-\eta$ plane, traffic hysteresis will be generated in the form of CW, CCW, or multiple loops. Empirical results suggest that the symmetry condition is not easy to satisfy and thus hysteresis loops (CW, CCW or multiple loops) are very commonly observed (see Figure 8). While it seems that a reaction pattern could generate infinite hysteresis cases, our empirical results reveal that only a handful are dominant as shown next.

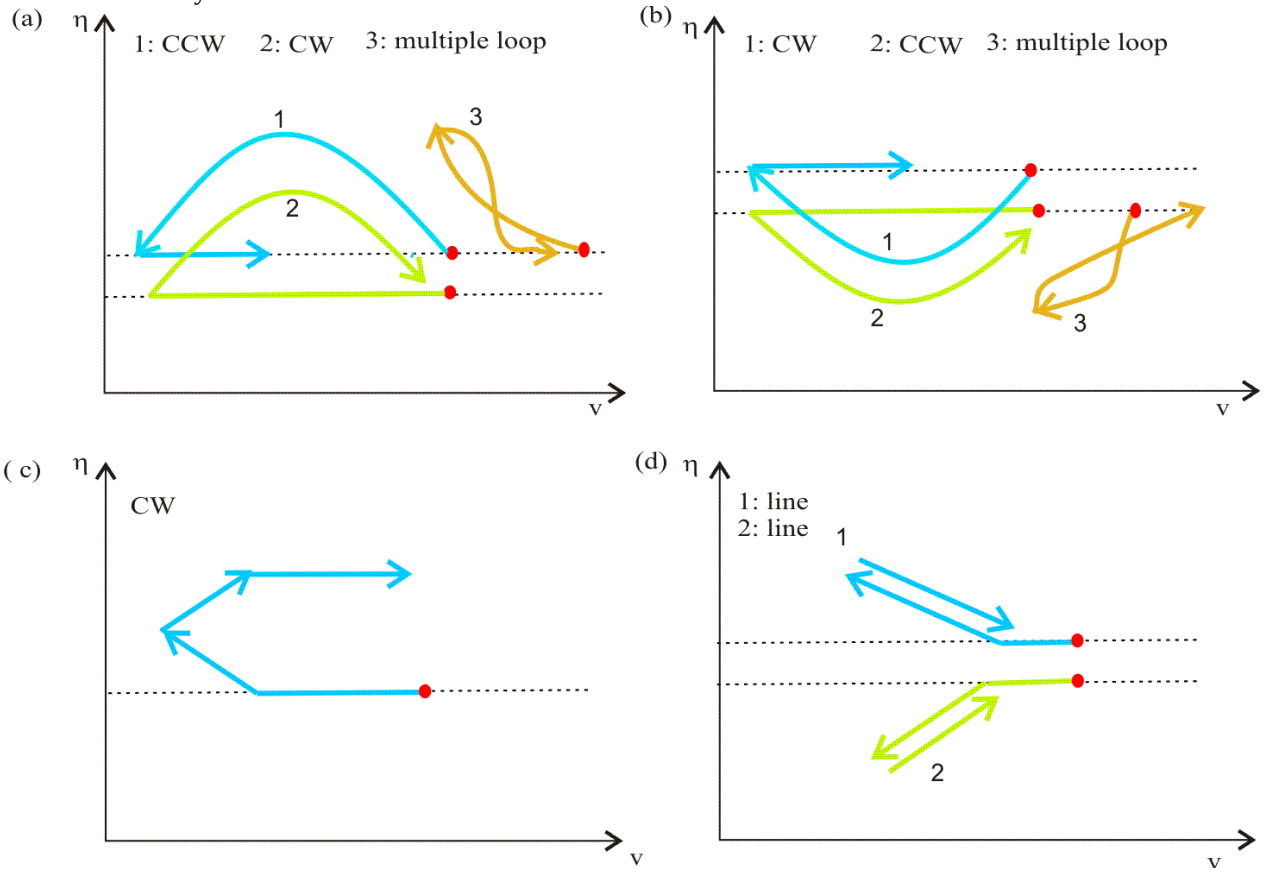

Figure 10 Relationship between reaction pattern and hysteresis type during an oscillation

6.2 Major mechanisms of generating traffic hysteresis

We define two response scenarios for drivers that adopt reaction patterns in oscillations:

(i) *early* response: $\eta_i(t)$ starts to deviate from η_i^0 around the beginning of the deceleration process of an oscillation cycle and recovers to η_i^1 before (or near) the start of the acceleration process;

(ii) *late* response: $\eta_i(t)$ starts to deviate from η_i^0 at (or around) the end of the deceleration process of an oscillation cycle and continues the change in the acceleration process.

The response scenario is a critical factor when causing traffic hysteresis. Investigation of trajectories that exhibited CW or CCW loops reveals that when drivers use reaction patterns in oscillations, they mainly fall in two response scenarios defined above.

We find that CW loops are mainly generated from the following two mechanisms: (1) generated from late-response concave and non-decreasing patterns (see Figure 11(a) and Figure 5, respectively); and (2) generated from early-response convex pattern (Figure 11(b)). Mechanism (1) is prevalent in both periods while a certain proportion (about 15%) of CW loops cases in the growth period follow mechanism (2). Interestingly, the CW loops caused by the two mechanisms are different. As illustrated in Figure 11(c), the region bounded by the loop can be above or below the driver's equilibrium level captured by η_i^0. In the former case the hysteresis is positive: the speed under hysteresis is greater than the equilibrium level. By contrast, the hysteresis is negative in the latter case. Thus, we use CW^+ and CW^- loop to distinguish the two cases.

The CCW loops are generated from two major mechanisms as well: (i) generated from early-response concave pattern (Figure 12(a)); and (ii) from late-response convex pattern (Figure 12(b)). Interestingly, most of the CCW loop cases in the growth period follow the second mechanism but accord well with the first one in the fully-developed period. Similar to the CW loops, CCW loops caused by the two mechanisms are different and can be denoted by CCW^+ and CCW^- loop, respectively.

(a)

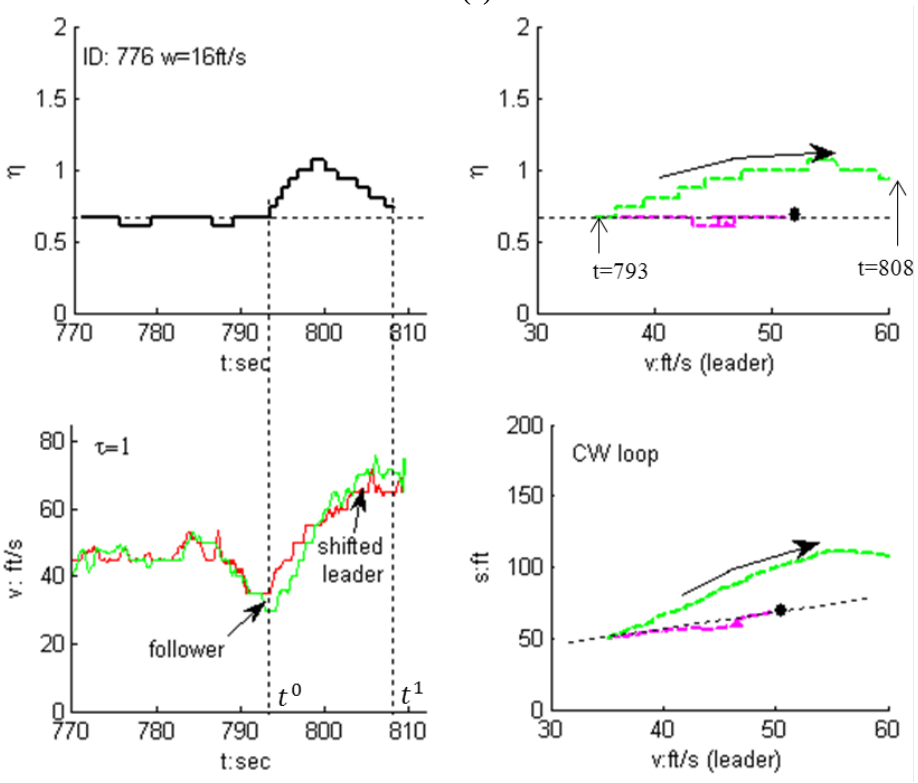

(b)

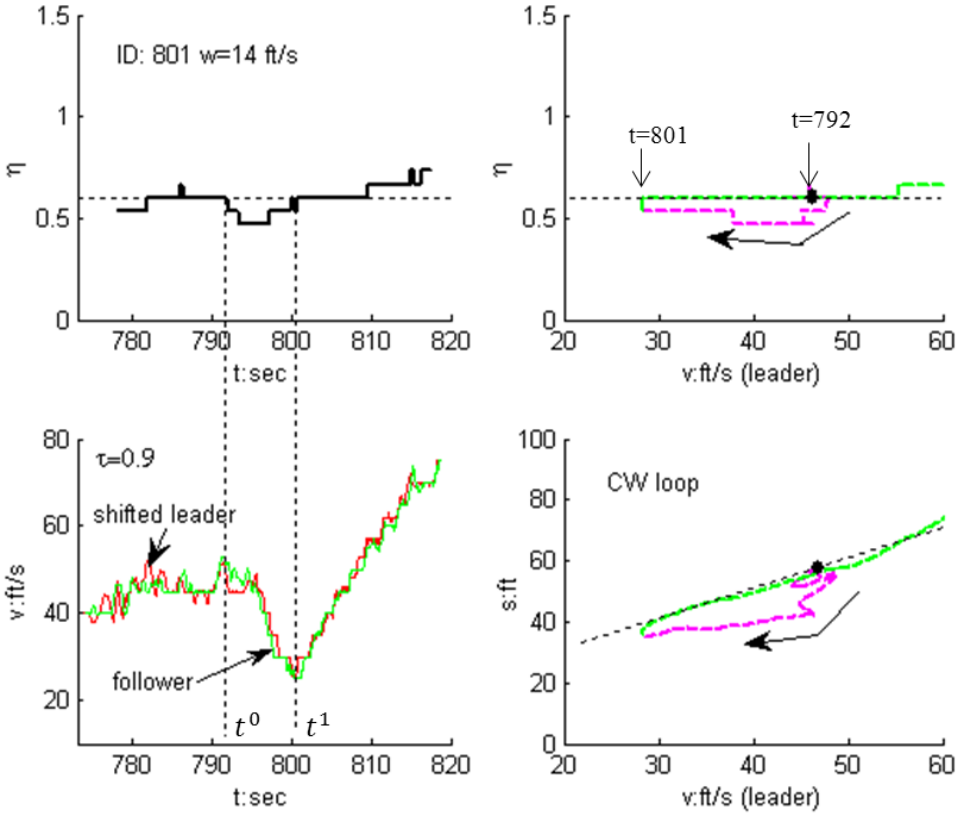

(c)

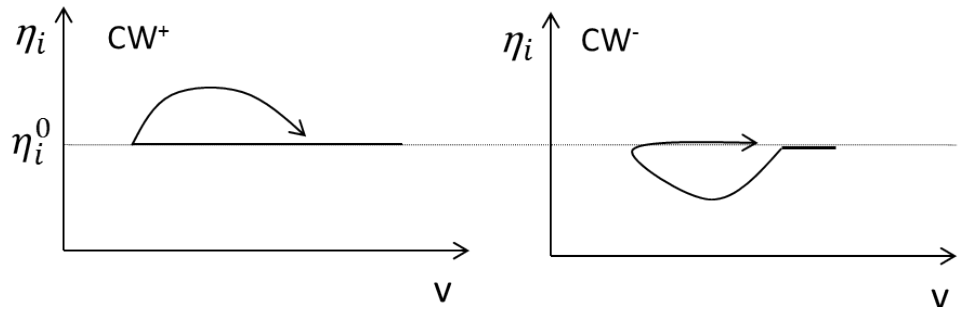

Figure 11 (a) Example of concave pattern with CW loop; (b) Example of convex pattern with CW loop; (c) Illustration of CW^+ and CW^- hysteresis loop

(a)

This is a draft version. Please cite it as: Chen, D., Laval, J., Ahn, S., Zheng, Z., 2012. Microscopic traffic hysteresis in traffic oscillations: a behavioral perspective. *Transportation Research Part B 46*(10), 1440-1453.

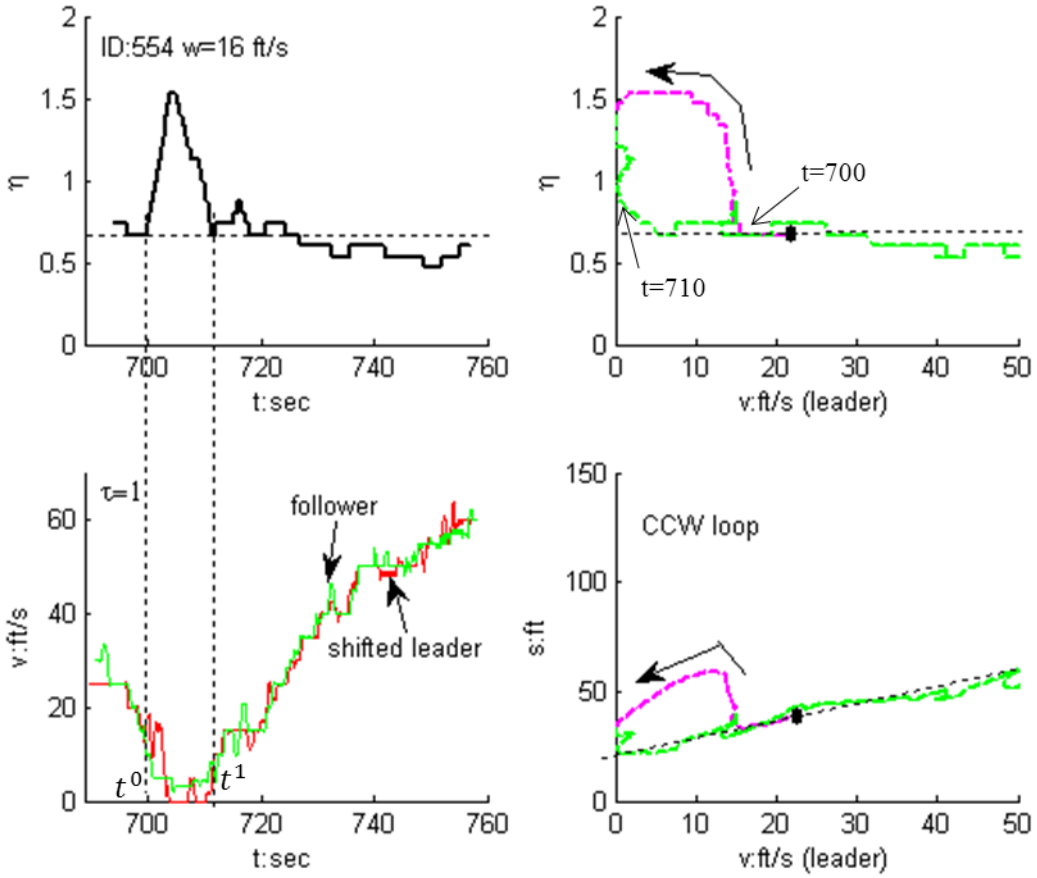

(b)

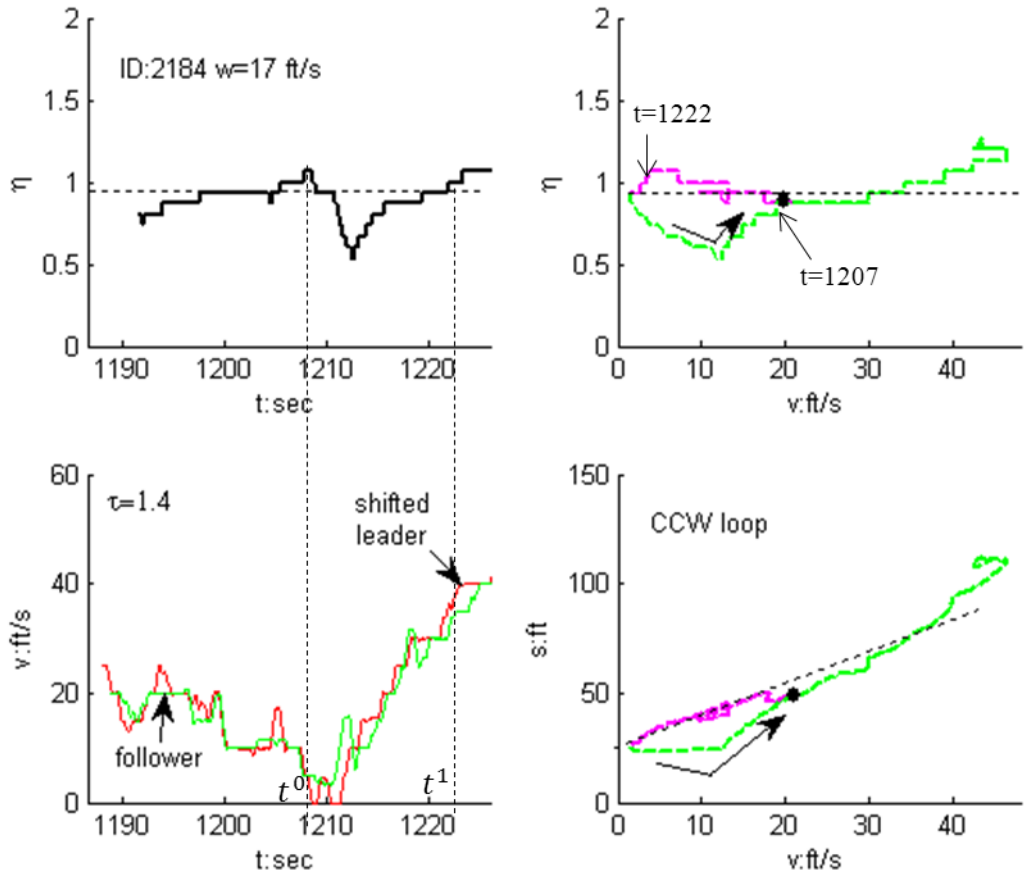

Figure 12 (a) Illustration of concave pattern with CCW loop; (b) Illustration of convex pattern with CCW loop.

6.3 Distribution of traffic hysteresis

The mechanisms of generating traffic hysteresis in the two periods are introduced by the following remarks with the frequency histogram shown in Figure 13:

R5: In growth period, OA drivers tend to have non-decreasing and concave patterns in late response scenario, which both cause CW^+ loops. In full-developed period, when using concave pattern, OA drivers have even probability to have early and late response, which results in CW^+ and CCW^+ loops, respectively.

R6: In both periods OT drivers tend to have convex pattern in the late response scenario and generate CCW^- loops.

R7: In growth period, ON drivers tend to have concave and non-decreasing patterns in late response scenario but convex pattern in early response scenario, which generates CW^+ loops and CW^- loops, respectively. In fully-developed period, ON drivers have comparable probability to have concave pattern in early and late response scenarios, which generates CW^+ and CCW^+ loops, respectively.

A summary of the results is provided in Table 4, in which the solid dots (circles) represent CW (CCW) loops and the size of the dots/circles qualitatively illustrates the frequency.

One can see that the distribution of hysteresis types is affected by three factors: (1) the distribution of driver category, (2) the preference of reaction pattern for each driver category, and (3) the response scenario used. Given that the distribution of driver categories is not significantly different (see R2), R4-7 suggest that (2) and (3) play a critical role in the hysteresis distribution change in the two periods. In particular, the increased proportion of CCW loops in the fully-developed period is the result of the increased number of concave pattern that occurs

in early response scenario, which is a compound effect of (i) the increased probability of OA and ON drivers to adopt concave pattern (see R3a & R3b) and (ii) the increased probability to have early response when they use concave pattern (see R5 and R7). Both (i) and (ii) suggest changes in driver behavior.

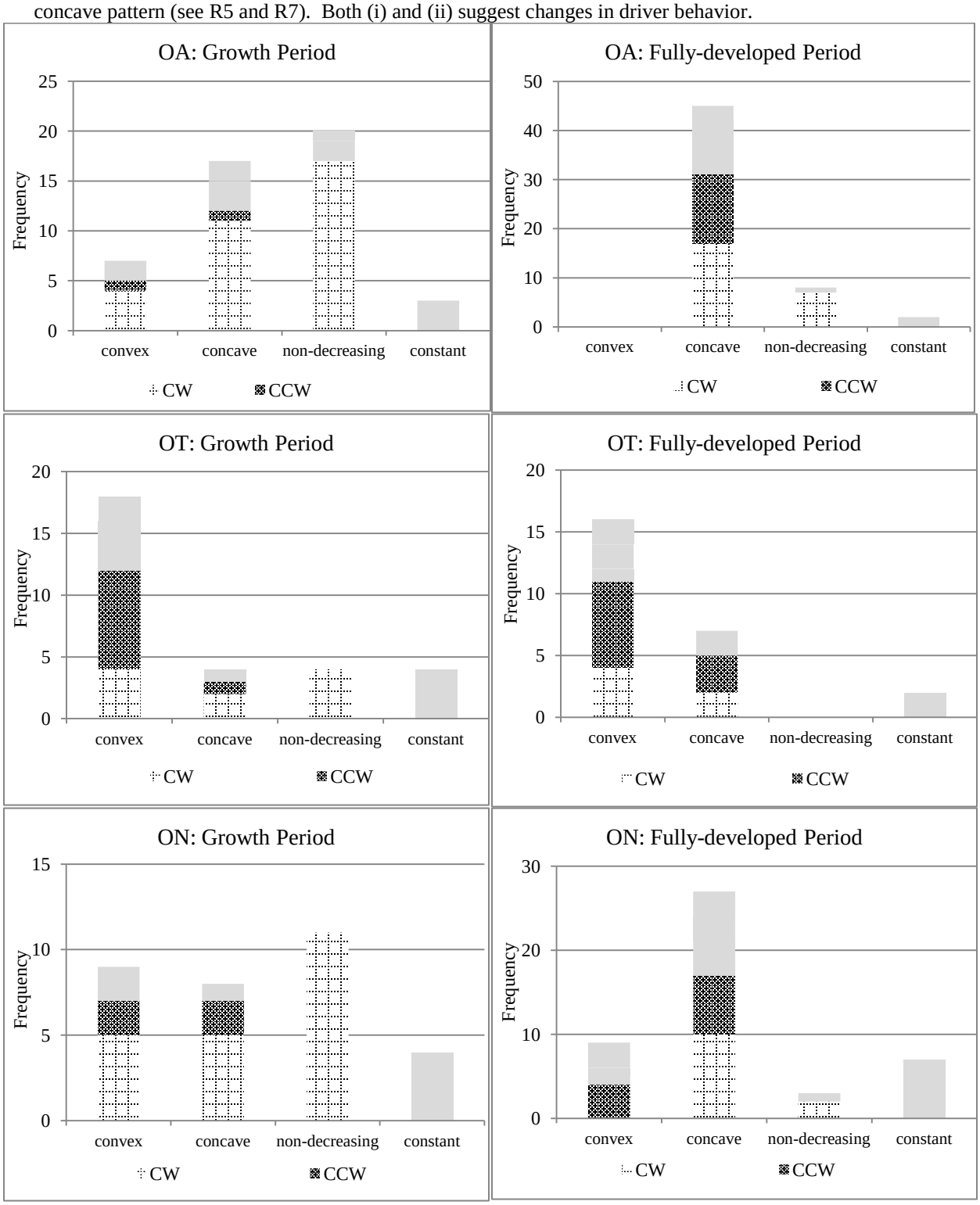

Figure 13 Driver category, behavior pattern and hysteresis pattern.

This is a draft version. Please cite it as: Chen, D., Laval, J., Ahn, S., Zheng, Z., 2012. Microscopic traffic hysteresis in traffic oscillations: a behavioral perspective. *Transportation Research Part B 46*(10), 1440-1453.

Table 4 Major hysteresis patterns for two periods

	OA					OT					ON				
	concave		n-d*	convex		concave		n-d	convex		concave		n-d	convex	
	early	late	Both	early	late	early	late	both	early	late	early	late	both	early	late
	CCW^+	CW^+	CW^+	CW^-	CCW^-	CCW^+	CW^+	CW^+	CW^-	CCW^-	CCW^+	CW^+	CW^+	CW^-	CCW^-
growth		●	●							○		●	●	●	
fully-developed	○	●								○	○	●			

○ : CCW
● : CW
*: n-d stands for non-decreasing pattern.

7 Discussions

This paper has investigated the traffic hysteresis arising in traffic oscillations from a behavioral perspective. Traffic hysteresis is connected to driver category and their reaction pattern to traffic oscillations by variable, $\eta_i(t)$. Our observations suggest that traffic hysteresis is generated when drivers' reaction to traffic oscillations is not symmetric on the $v-\eta$ plane.

From a modeling perspective, our findings indicate that the oscillation development stage should be taken into account when modeling driver's car-following behavior. Our statistical results suggest that driver behavior varies with the development stage of traffic oscillations. In particular, drivers' preference of reaction pattern and response scenario varies in different development stages. In order to take the behavior change into account in a simulation model, one possibility is to evaluate the leader's speed as a proxy for the oscillation development stage. For example, once the leader's speed reaches zero the oscillation stage is fully-developed while before that instance the stage is growth. We also find it necessary to capture the response scenario when describing driver's car-following behavior because that will affect the traffic hysteresis generated. Fortunately, our empirical results suggest that the reaction patterns mainly occur in two response scenarios, early or late response. Therefore, one may assume that early response is initiated whenever the deceleration wave is triggered and the late response starts at the beginning of the acceleration process. This can be included in the behavioral model without adding additional parameters.

The procedure for numerical simulation is presented in Figure 14. Driver behavior is determined in four layers: (i) the proportion of each driver category (OA, ON, OT), (ii)the stage of traffic oscillations (growth or fully-developed), (iii) the probability of reaction patterns (concave, convex, constant, or non-decreasing) that each driver category will adopt, which depends on the development stage of traffic oscillations, and (iv) the response scenario (early or late reaction pattern). The probabilities in each layer can be taken from empirical measurement presented here.

Notice that (1) driver category, (2) reaction pattern, and (3) response scenario are all correlated and the relationship depends on the (4) development stage of traffic oscillations. In Chen, et al. (2012), the correlation between (1) and (2) is captured using sample enumeration for the five-parameter set $[\eta_i^0, \eta_i^T, \eta_i^1, \varepsilon_i^0, \varepsilon_i^1]$. Our statistical results suggest that this correlation is correlated with (4), but it is unclear at this point whether the joint distribution of the parameter set is independent of (3). This problem is important when generating parameters in simulations. Further measurement and statistical test are needed.

Finally, it is worth noting that the non-decreasing pattern suggests that drivers increases their equilibrium spacing level but do not return to the preferred level before oscillations. We agree with Chen, et al. (2012) that this may be because the trajectories are not long enough to cover the recovery. Notice that this pattern is very common in the growth period and plays an important role in producing CW loops. The hysteresis resulting from this pattern is quite significant, and the difference of spacing for a given speed may be up to 70 feet (see Figure 5 (d)). Interestingly, its mechanism in generating CW loops is very similar to the concave pattern. Thorough investigation based on extensive trajectories is needed.

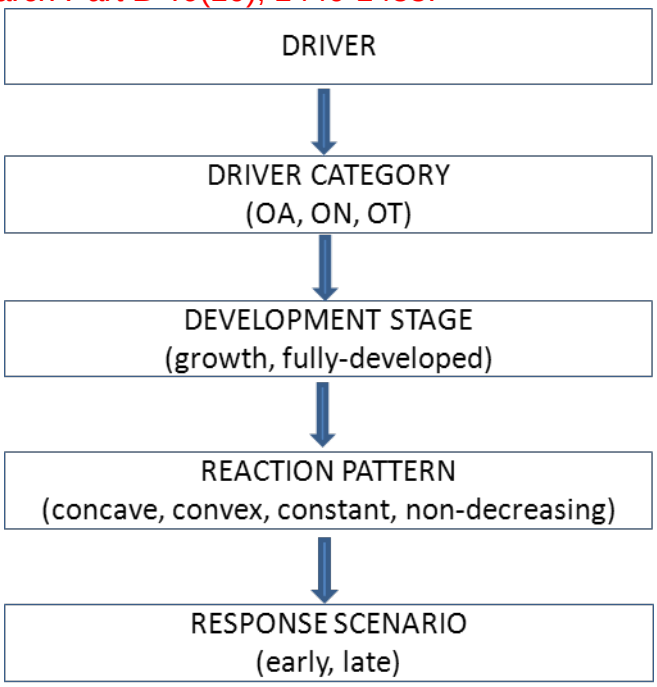

Figure 14 Procedure for driver behavior modeling.

Acknowledgement

This research was funded by National Science Foundation.

References

Ahn, S., Vadlamani, S., Laval, J.A., Chen, D., 2011. A method to account for non-steady conditions in measuring traffic hysteresis. Transportation Research Part B. In Press.

Chen, D., Laval, J.A., Zheng, Z., Ahn, S., 2012. Traffic oscillations: a behavioral car-following model. Transportation Research Part B 978. In Press.

Durent, A., Ahn, S., Buisson, C., 2011. Passing rates to measure relaxation and impact of lane-changing in queue. Computeraided engineering and infrastructure engineering 26 (4), 285-297.

Edie, L.C., 1961. Car-Following and Steady-State Theory for Noncongested Traffic. Operations Research 9(1), 66-76.

Greenwood, P.E., Nikulin, M.S., 1996. A guide to chi-squared testing. Wiley-Interscience (1 edition).

Laval, J.A., 2010. Hysteresis in traffic flow revisited: An improved measurement method. Transportation Research Part B 45(2), 385-391.

Laval, J.A., Leclercq, L., 2010. A mechanism to describe the formation and propagation of stop-and-go waves in congested freeway traffic. Philosophical Transactions of the Royal Society A: Mathematical, Physical and Engineering Sciences 368 (1928), 4519-4541.

Lighthill, M.J., Whitham, G.B., 1955. On Kinematic Waves. I. Flood Movement in Long Rivers. Proceedings of the Royal Society of London. Series A. Mathematical and Physical Sciences 229(1178), 281-316.

Maes, W., 1979. Traffic data collection system for the Belgian motorway network-measures of effectiveness aspects. Proceedings of the International Symposium on Traffic Control Systems. 2D-Analysis and Evaluation, 45-73.

Newell, G.F., 1965. Instability in dense highway traffic, a review. The 2nd International Symposium on Transportation and Traffic flow Theory (ed J. Almond), 73-83.

Newell, G.F., 2002. A simplified car-following theory: a lower order model. Transportation Research Part B 36(3), 195-205.

NGSIM, 2006. Next generation simulation. http://ops.fhwa.dot.gov/trafficanalysistools/ngsim.htm.

Ngoduy, D., 2011. Multiclass first-order traffic model using stochastic fundamental diagrams. Transportmetrica, 7, 111-125.

Richards, P.I., 1956. Shock Waves on the Highway. Operations research 4(4), 42-51.

Treiterer, J., Myers, J.A., 1974. The hysteresis phenomenon in traffic flow. The 6th International Symposium on Transportation and Traffic flow Theory, 13-38.

Wong G.C.K. and Wong S.C., 2002. A multi-class traffic flow model - an extension of LWR model with heterogeneous drivers. Transportation Research Part A, 36, 827-841.

Yeo, H., Skabardonis, A., 2009. Understanding stop-and-go traffic in view of asymmetric traffic theory. The 18th International Symposium on Transportation and Traffic flow Theory. (ed. by W. Lam, S.C. Wong & H. Lo) 1, 99-116.

Zhang, H.M., 1999. A mathematical theory of traffic hysteresis. Transportation Research Part B 33(1), 1-23.

Zhang, H.M., Kim, T., 2005. A car-following theory for multiphase vehicular traffic flow. Transportation Research Part B 39(5), 385-399.